Original Article

DOI: 10.5582/ddt.2024.01070

Mitotic abnormalities and spindle assembly checkpoint inactivation in a cell model of Shwachman-Diamond syndrome with mutations in the Shwachman-Bodian-Diamond syndrome gene, 258+2T > C

Yukihiro Sera, Tsuneo Imanaka*, Yusuke Iguchi, Masafumi Yamaguchi

Laboratory of Physiological Chemistry, Faculty of Pharmaceutical Sciences, Hiroshima International University, Hiroshima, Japan.

SUMMARY Hematologic abnormalities are the most common symptoms of Shwachman-Diamond syndrome (SDS). The causative gene for SDS is the Shwachman-Bodian-Diamond syndrome (*SBDS*) gene; however, the function of SBDS and pathogenesis of each condition in SDS are largely unknown. SBDS is known to be localized at mitotic spindles and stabilizes microtubules. Previously, we demonstrated that SBDS is ubiquitinated and subsequently degraded in the mitotic phase, thereby accelerating mitotic progression. In this study, we examined mitosis in a myeloid cell model of SDS (SDS cells). 4',6-Diamidino-2-phenylindole (DAPI)-stained chromosome observation and cell cycle analysis of nocodazole-synchronized cells revealed that the SDS cells have abnormally rapid mitosis. In addition, many lagging chromosomes and micronuclei were detected. Moreover, the phosphorylation of threonine tyrosine kinase, the crucial kinase of the spindle assembly checkpoint (SAC), was suppressed. Chromosomal instability caused by SAC dysfunction may cause a variety of clinical conditions, including hematologic tumors in patients with SDS.

Keywords Shwachman-Diamond syndrome, mitosis, chromosomal instability, spindle assembly checkpoint

1. Introduction

Shwachman-Diamond syndrome (SDS) is an autosomal recessive inherited disorder characterized by bone marrow failure and exocrine pancreatic insufficiency (*1*). Neutropenia is present in almost all patients with SDS and can lead to serious infections, including sepsis. In addition, SDS is associated with other life-threatening complications such as myelodysplastic syndrome (MDS) and acute myeloid leukemia (AML) (*2-4*). Patients with SDS usually present in infancy and have an average life expectancy of 30-40 years; however, the life expectancy of patients with hematologic disorders, such as those aforementioned, is significantly shorter (*5,6*).

The causative gene for SDS is the highly conserved Shwachman-Bodian-Diamond syndrome (*SBDS*) gene on chromosome 7 (*7*). The most widely accepted function of SBDS is ribosome biogenesis and ribosomal RNA metabolism (*8,9*). In addition, SBDS is reportedly involved in several biological processes including cellular stress responses, proliferation, and differentiation (*10-12*). SBDS has also been implicated in mitosis. Austin *et al*. showed that SBDS localizes to mitotic spindles and stabilizes microtubules (*13*). In addition, Orelio *et al.* showed the similar mitotic localization of SBDS, which may be associated with cell proliferation (*14*). Furthermore, we previously showed that SBDS colocalizes with ring finger protein 2 (RNF2) on centrosomal microtubules in the mitotic phase (M phase) and that the ubiquitination and degradation of SBDS by RNF2 accelerate mitotic progression (*15,16*). However, the precise role of SBDS remains unknown.

To elucidate the function of SBDS and the pathogenesis of SDS, we established a cell model of SDS harboring a common *SBDS* variant at intron 2, 258+2T > C, using a murine myeloid cell line (*17*). The mutation results in an aberrant splicing at position 251-252, which generates a premature termination codon in the mRNA of SBDS and consequently produces a truncated, non-functional protein. We examined the cell division process and found that mitosis was abnormally rapid in these cells. In addition, many lagging chromosomes and micronuclei were detected. Furthermore, the spindle assembly checkpoint (SAC), which is essential for proper chromosome segregation, was inactivated. As improper chromosome segregation is associated with DNA

damage, cell death, and tumor cell malignancy, failure of this mitotic checkpoint may be a key factor in various hematologic conditions such as neutropenia, AML, and MDS in patients with SDS.

2. Materials and Methods

2.1. Antibodies, reagents

Anti-SBDS antiserum was prepared as previously described (*18*). Anti-cyclin B1 antibody (sc-245) and anti-pituitary tumor-transforming gene (PTTG) antibody (sc-56207) were obtained from Santa Cruz Biotechnology (Dallas, TX, USA). Anti-threonine tyrosine kinase (TTK) (phospho Thr676) antibody was from Wuhan Huamei Biotech (CSB-PA060023; Wuhan, Hubei, China). Anti-TTK antibody was from Affinity Biosciences (DF6969; Cincinnati, OH, USA). Anti-phospho-Ser/Thr-Pro mitotic protein monoclonal 2 (MPM-2) antibody (anti-MPM-2 antibody) was from Sigma (05-368; St. Louis, MO, USA). Anti-α-tubulin antibody (017-25031) and anti-β-actin antibody (281-98721) were from Wako Chemicals (Osaka, Osaka, Japan). The secondary antibodies for immunofluorescence were anti-rabbit IgG-FITC (sc-2012; Santa Cruz Biotechnology) and anti-mouse IgG-rhodamine (55539; Cappel Laboratories, Malvern, PA, USA). Nocodazole (NCZ; 036-18371) was from Wako Chemicals.

2.2. Cell culture

32Dcl3 cells were cultured in Iscove's Modified Dulbecco's Medium supplemented with fetal bovine serum and WEHI-3b conditioned medium (*16*). 32Dcl3 cell model of SDS (SDS cells) was established as previously described (*17*). SDS cells were transfected with pcDNA3.1/Flag-SBDS *via* electroporation, as required. The synchronization of cells to the G2/M phase was achieved through the overnight culturing of cells in the presence of 100 ng/mL NCZ.

2.3. Immunofluorescence and chromosome staining

Cells were attached to a microscope slide and subsequently fixed, permeabilized, and stained in accordance with the previously described procedure (*16*). Images were obtained using the LSM800 confocal microscope (Carl Zeiss Microscopy, White Plains, NY, USA).

2.4. Cell cycle analysis

Cell cycle analysis was performed as previously described (*16*). In brief, DNA in fixed cells was stained with propidium iodide (Wako Chemicals). DNA content was measured using the FACSCalibur flow cytometer (BD Biosciences, Franklin Lakes, NJ, USA).

2.5. Immunoblotting

Cells were lysed in extraction buffer (20 mM Tris-HCl, pH 7.5, 150 mM NaCl, 1 mM EDTA, 100 μM sodium orthovanadate, 1% NP-40, 2 μM leupeptin, 2 μM pepstatin A, 1 mM phenylmethylsulfonyl fluoride, 5 nM calyculin A). Lysates were centrifuged at 20,000 *g* for 15 min at 4°C to remove debris. The cell extract was denatured by heating to 55°C for 10 min in sodium dodecyl sulfate loading buffer (50 mM Tris-HCl, pH 6.8, 100 mM dithiothreitol, 2% sodium dodecyl sulfate, 0.1% bromophenol blue, 10% glycerol), separated by sodium dodecyl sulfate-polyacrylamide gel electrophoresis, and electrotransferred to polyvinylidene fluoride membranes. The membranes were blocked in 1% bovine serum albumin in tris-buffered saline with Tween 20 (200 mM NaCl, 20 mM Tris-HCl, 0.05% Tween 20, pH 7.5), and then incubated with primary antibodies followed by horseradish peroxidase-conjugated anti-immunoglobulin secondary antibodies.

2.6. Micronucleus assay

Cells were treated with 100 ng/mL NCZ for 16 h to induce micronuclei. The cells were deposited to a slide glass by centrifugation at 40 *g* for 5 min (StatSpin Cytofuge 2; StatSpin, Norwood, MA, USA). Cell fixation, permeabilization, and staining of chromosomes were performed as for immunofluorescence. Images were acquired on the LSM800 confocal microscope (Carl Zeiss Microscopy). Nuclei that are completely independent of the main nucleus and sufficiently small compared to the main nucleus were identified as micronuclei.

3. Results

3.1. Abnormally rapid M phase progression in SDS cells

We previously reported an association between SBDS degradation and mitotic progression (*16*) . Therefore, we examined the mitotic progression of the myeloblastic 32Dcl3 cell model of SDS harboring a common pathogenic *SBDS* variant in both alleles at intron 2, 258+2T > C (SDS cells). Wild-type (WT) and SDS cells were synchronized at the G2/M phase by NCZ treatment and collected every 15 min during mitosis. Cell cycle progression was analyzed by chromosome observation and flow cytometry analysis of DNA content. The observation of 4',6-diamidino-2-phenylindole (DAPI)-stained chromosomes revealed that SDS cells transitioned to anaphase earlier than WT cells (Figure 1A). Following the removal of NCZ, 51% of SDS cells had progressed to anaphase after 30 min, compared to 26% of WT cells (Figure 1B). Although no significant differences were obtained because the degree of progression of the mitotic phase differed in each experiment, the observed

trend exhibited a consistent pattern across all three experiments (Figure S1, *https://www.ddtjournal.com/action/getSupplementalData.php?ID=218*). Consistent with this result, SDS cells transitioned to G1 phase faster than WT cells after NCZ removal (Figure 1C and Figure S2, *https://www.ddtjournal.com/action/getSupplementalData.php?ID=218*). These results demonstrated that SDS cells had an abnormally rapid mitosis.

Another notable finding was that SDS cells exhibited incomplete G2/M arrest when treated with NCZ. Most WT cells treated with 100 ng/mL NCZ for 16 h stopped at the G2/M phase and only 1.25% of cells leaked into the G1 phase, whereas 3.97% of SDS cells leaked into the G1 phase (Figure S3, *https://www.ddtjournal.com/action/getSupplementalData.php?ID=218*). In addition, at 24 h after NCZ removal, many WT cells remained in the G2/M phase, whereas most SDS cells had already returned to the normal cell cycle (Figure S2, *https://www.ddtjournal.com/action/getSupplementalData.php?ID=218*). These findings indicate a reduced sensitivity to NCZ in SDS cells.

3.2. Chromosomal instability in SDS cells

In the previous chromosome observation experiment, we observed lagging chromosomes. This finding prompted us to determine the frequency of lagging chromosomes in mitosis. It has been reported that the formation of lagging chromosomes is enhanced in cells released from NCZ treatment (*19*). Indeed, several lagging chromosomes were observed during the chromosome observation experiment. Briefly, WT and SDS cells were synchronized at the G2/M phase by treatment with 100 ng/mL NCZ for 13 h, and then released into fresh medium. To recover the anaphase cells, SDS cells were collected 30 min after release from the NCZ block, and WT cells were collected 15 min later. Then DAPI-stained chromosomes were observed together with immunostained microtubules (Figure 2A). Cells undergoing chromosome segregation were counted to determine the percentage of cells with lagging chromosomes. Lagging chromosomes were observed in about half of the anaphase SDS cells and were almost twice as frequent in SDS cells as in WT cells (Figure 2B). Chromosomal instability seems to be increased in SDS cells.

3.3. SAC inactivation in SDS cells

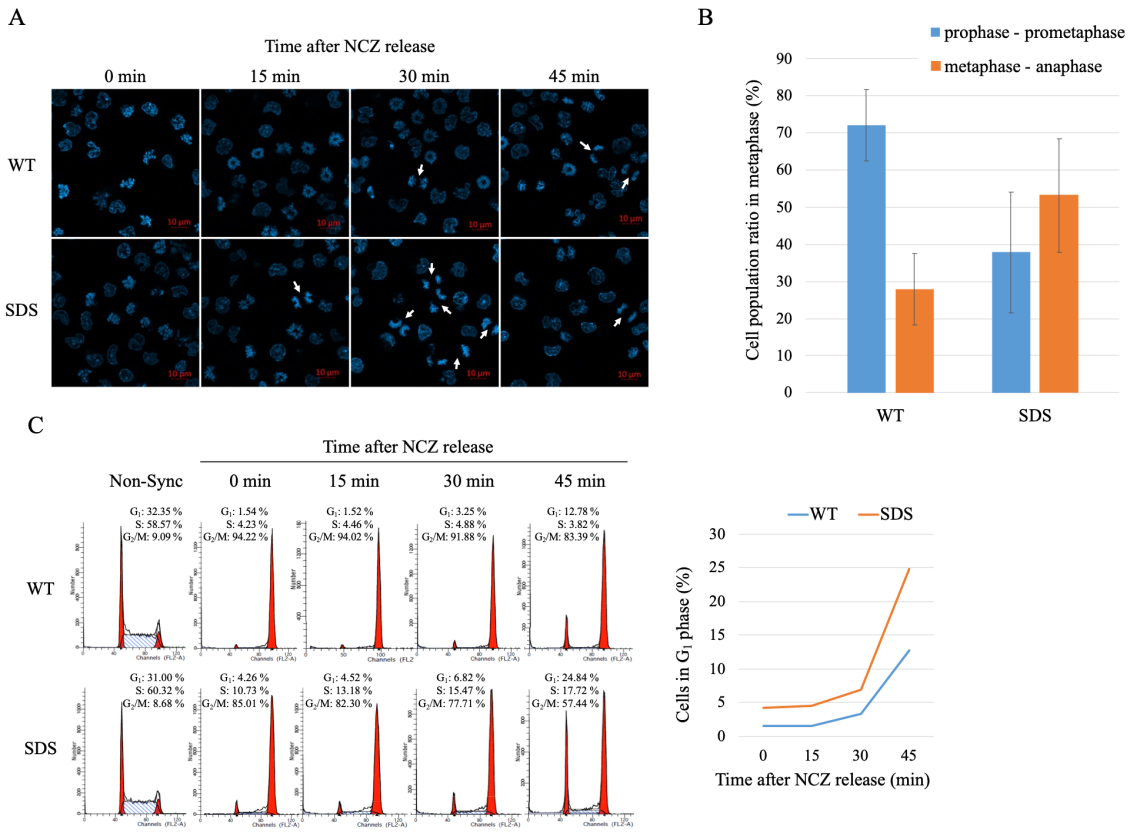

Figure 1. Abnormally rapid M phase progression in SDS cells. Cells were synchronized at the G2/M phase by treating with NCZ for 13 h, released into fresh medium, and harvested at the indicated time. **(A)** DAPI-stained chromosome observation. Prophase, in which chromosomes are cohesive; prometaphase, in which chromosomes are aligned in a ring; and anaphase, in which chromosomes are segregating (white arrows). **(B)** More than 50 mitotic cells were observed and the ratio of pre-metaphase to post-metaphase cells was calculated. The experiment was repeated three times. **(C)** Cell cycle analysis with propidium iodide. The percentage of cells transitioning from the M to G1 phase after NCZ removal was analyzed over time.

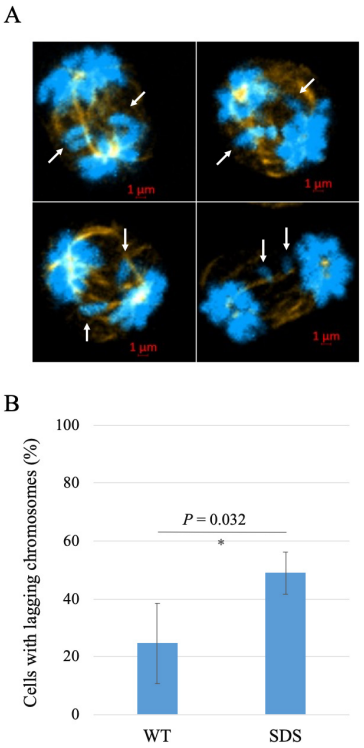

Figure 2. Increased frequency of NCZ-induced lagging chromosomes in SDS cells. (A) Lagging chromosomes (white arrows) detected in SDS cells after release from NCZ. **(B)** Approximately 50 anaphase cells were observed and the frequency of lagging chromosomes was calculated. The experiment was repeated three times.

NCZ, an inhibitor of microtubule polymerization, activates SAC and induces G2/M arrest in cells (*20*). The abnormally rapid mitosis, reduced sensitivity to NCZ, and especially, the increased number of lagging chromosomes led us to hypothesize that SAC may not be functioning properly in SDS cells. SAC monitors the attachment of spindle microtubules to kinetochores. Once the nuclear membrane disappears, the SAC leader kinase, TTK/monopolar spindle kinase 1, localizes to the kinetochore and is activated by autophosphorylation (*21*). Activated TTK on the unattached kinetochores phosphorylates a number of substrates and triggers the accumulation of SAC proteins, leading to formation of the mitotic checkpoint complex (MCC). MCC inhibits the anaphase-promoting complex/cyclosome (APC/C) E3 ubiquitin ligase. Once the SAC is satisfied, the APC/C is activated and initiates chromosome segregation through ubiquitination-mediated degradation of PTTG1/securin and cyclin B1 (*22*). First, we examined the activation of TTK in cells treated with NCZ. TTK phosphorylation was enhanced after NCZ treatment of WT cells, whereas it was drastically suppressed in SDS cells (Figure 3A). A similar trend was observed for the amounts of M phase-specific phosphoproteins recognized by the anti-MPM-2 antibody (Figure 3B). In addition, the substrates of APC/C, namely, PTTG1 and cyclin B1, were decreased from early mitosis in SDS cells (Figure 3C). These results suggest that SAC activation is attenuated in SDS cells.

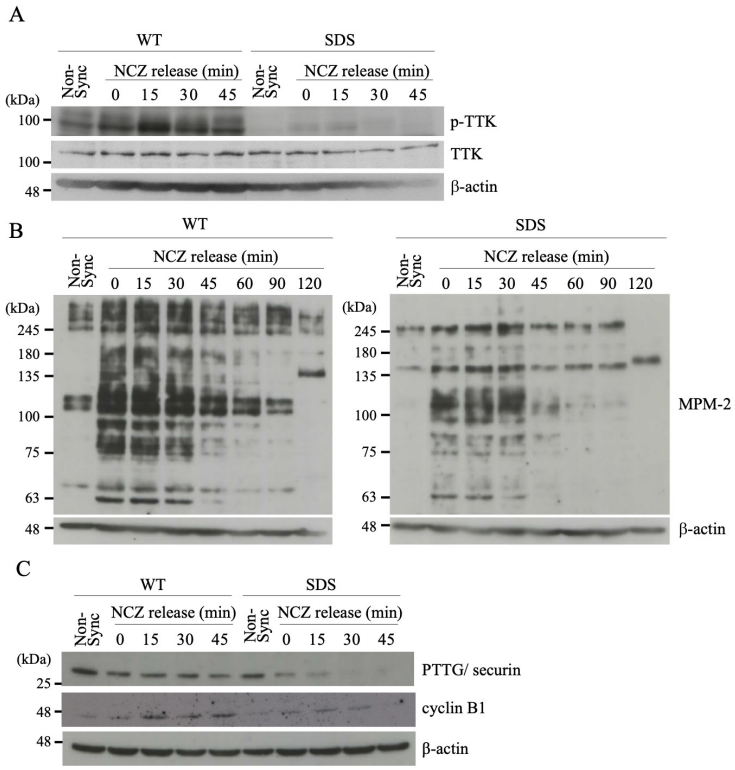

Figure 3. SAC inactivation in SDS cells. Cells were synchronized with NCZ treatment and harvested at the indicated time after release from NCZ. **(A)** Phosphorylated TTK, the master kinase in SAC, **(B)** a variety of mitosis-specific phosphoproteins detected by anti-MPM-2 antibody, and **(C)** PTTG/securin and cyclin B1, representative substrates of APC/C, were detected by immunoblotting.

3.4. SBDS required for SAC activation

SDS cells have mutations in the *SBDS* gene, resulting in a substantial reduction of SBDS protein expression. We overexpressed Flag-SBDS in SDS cells. Re-expression of SBDS in SDS cells increased the phosphorylation of TTK and other mitotic proteins upon NCZ treatment (Figure 4A). In addition, the abnormally rapid mitosis and reduced sensitivity to NCZ were improved (Figure 4B). Lagging chromosomes that are not incorporated into the main nucleus form micronuclei. In accordance with the observed increase in lagging chromosomes (Figure 2), the formation of micronuclei was also elevated in SDS cells, which was suppressed by the re-expression of SBDS in SDS cells (Figures 4C and 4D). These results indicate that SBDS is essential for proper functioning of the SAC. In addition, the mitotic localization of SBDS was examined in detail. The WT 32Dcl3 cells were harvested every 15 min after release from NCZ block and immunostained with the appropriate antibodies. Consistent with our report and others (*13,14,16*), SBDS was localized to the nucleolus in interphase and to the mitotic spindles in the M phase. The mitotic localization was stronger from prometaphase to metaphase and weaker in anaphase (Figure S4, *https://www.ddtjournal.com/action/getSupplementalData.php?ID=218*). This change in SBDS localization coincides with the timing of SAC activation and inactivation, suggesting that SBDS coordinates with SAC activation.

4. Discussion

This is the first study to present evidence showing the inactivation of SAC in SBDS-downregulated cells and the involvement of SBDS in SAC activation. In 2008, localization of SBDS to the mitotic spindles and its contribution to the stabilization of the mitotic spindles were shown for the first time, but the contribution of SBDS to SAC was unclear as the cells lacking SBDS were arrested at the G2/M phase by treatment with NCZ, an activator of SAC (*13*) . In our study, SDS cells with mutations in both *SBDS* alleles were also synchronized to the G2/M phase by NCZ treatment, but a fraction of the cells leaked into the G1 phase during G2/M arrest (Figure S3, *https://www.ddtjournal.com/action/getSupplementalData.php?ID=218*). In addition,

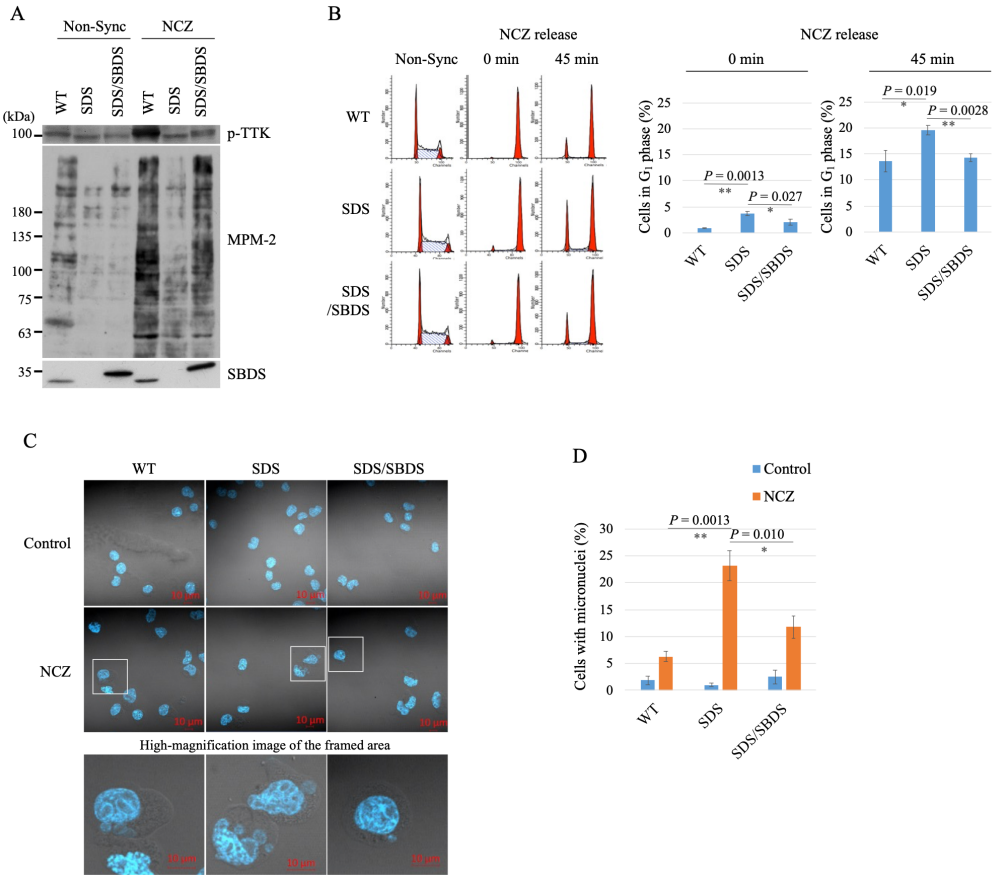

Figure 4. Re-expression of SBDS reactivates the SAC and normalizes mitosis in SDS cells. (A) Immunoblot analysis of phosphorylated TTK and mitosis-specific phosphoproteins detected by anti-MPM-2 antibody in WT, SDS, and SDS/SBDS cells. **(B)** Assessment of mitotic progression and NCZ sensitivity by cell cycle analysis. NCZ sensitivity was assessed by the percentage of cells that leaked into the G1 phase under G2/M arrest by NCZ treatment (NCZ release 0 min), and mitotic progression was assessed by the percentage of cells that transited to the G1 phase 45 min after release from NCZ block. **(C, D)** Evaluation of genomic instability by micronucleus assay. More than 100 cells were observed and the experiment was repeated three times.

after NCZ removal, the SDS cells immediately entered anaphase and then the G1 phase compared to WT cells (Figure 1). Furthermore, more lagging chromosomes were detected in the SDS cells (Figure 2). These results suggest that SAC, the surveillance mechanism to delay mitotic progression for accurate chromosome segregation, is not functioning properly in SDS cells. This is also supported by the fact that SDS cells returned to the normal cell cycle sooner than WT cells after NCZ removal (Figure S2, *https://www.ddtjournal.com/action/getSupplementalData.php?ID=218*). Indeed, the activation of TTK, the leader kinase of SAC, was suppressed in SDS cells (Figure 3A). These findings are consistent with the report that SAC inactivation through TTK inhibition significantly decreases the mitotic delay caused by NCZ treatment (*23*).

The SAC monitors microtubule attachment to the kinetochore and arrests the metaphase-anaphase transition until all microtubules have attached to the kinetochore (*24*). Therefore, an incomplete SAC leads to chromosome missegregation, which in turn leads to genomic instability and tumorigenesis. Mutations in SAC genes and alterations in the protein levels of SAC proteins have been reported in several human tumors including T-cell leukemia/lymphoma, B-cell lymphoma, and AML (*25-27*), which are often associated with SAC impairment, chromosomal instability, and even aneuploidy. Genomic instability has been found in primary bone marrow stromal cells derived from patients with SDS as well our established SDS cell model (*13*). In addition, hematologic malignancies such as AML and MDS are serious complications of SDS. SAC inactivation may contribute to genomic instability and tumorigenesis in SDS.

Most patients with SDS have variants of *SBDS*. The most common combination of mutations is 183-184TA>CT/ 258+2T>C (50%), followed by the 258+2T>C/ missense mutation (27.8%) (*7*) . The mutations result in a decrease of SBDS protein. Although little is known about the function of SBDS, it is well known that SBDS is localized to the nucleolus for the assembly of mature ribosomes and ribosome biogenesis in the interphase. SBDS binds to microtubules and stabilizes the mitotic spindles in the M phase. In addition, here we revealed that SBDS is localized to the mitotic spindles, particularly in the prometaphase to metaphase interval, which is associated with the activation of SAC (Figure S4, *https://www.ddtjournal.com/action/getSupplementalData.php?ID=218*). SBDS may support the activation of SAC by stabilizing microtubules and inhibiting the initiation of chromosome segregation until all of the spindles are bound to the chromosomes. On the other hand, the interaction between SBDS and M phase-specific polo-like kinase 1 (PLK1)-interacting protein (MPLKIP) has been reported (*28*). PLK1, the mitotic binding partner of MPLKIP, is a kinase that phosphorylates TTK and other SAC proteins to promote SAC signaling. SBDS may regulate PLK1 activity through the SBDS-MPLKIP-PLK1 interaction. At present, it is unclear whether there is a link between spindle stabilization and SAC activation.

In conclusion, we found that SAC does not function properly in SDS cells, resulting in chromosomal instability. Additionally, our results also suggest that SBDS contributes to SAC activation by some mechanism. Further studies focusing on this mitotic checkpoint, which is essential for chromosome stability, may help elucidate the pathogenesis of neutropenia, AML, and MDS, which are important pathological conditions in SDS. Our findings provide new perspectives for therapeutic drug development in SDS.

Funding: None.

Conflict of Interest: The authors have no conflicts of interest to disclose.

References

1. Shwachman H, Diamond LK, Oski FA, Khaw KT. The syndrome of pancreatic insufficiency and bone marrow dysfunction. J Pediatr. 1964; 65:645-663.
2. Woods WG, Roloff JS, Lukens JN, Krivit W. The occurrence of leukemia in patients with the Shwachman syndrome. J Pediatr. 1981; 99:425-428.
3. Dror Y, Squire J, Durie P, Freedman MH. Malignant myeloid transformation with isochromosome 7q in Shwachman-Diamond syndrome. Leukemia. 1998; 12:1591-1595.
4. Donadieu J, Leblanc T, Bader Meunier B, *et al*. Analysis of risk factors for myelodysplasias, leukemias and death from infection among patients with congenital neutropenia. Experience of the French Severe Chronic Neutropenia Study Group. Haematologica. 2005; 90:45-53.
5. Furutani E, Liu S, Galvin A, *et al*. Hematologic complications with age in Shwachman-Diamond syndrome. Blood Adv. 2022; 6:297-306.
6. Myers KC, Furutani E, Weller E, *et al.* Clinical features and outcomes of patients with Shwachman-Diamond syndrome and myelodysplastic syndrome or acute myeloid leukaemia: a multicentre, retrospective, cohort study. Lancet Haematol. 2020; 7:e238-e246.
7. Boocock GR, Morrison JA, Popovic M, Richards N, Ellis L, Durie PR, Rommens JM. Mutations in *SBDS* are associated with Shwachman-Diamond syndrome. Nat Genet. 2003; 33:97-101.
8. Ganapathi KA, Austin KM, Lee CS, Dias A, Malsch MM, Reed R, Shimamura A. The human Shwachman-Diamond syndrome protein, SBDS, associates with ribosomal RNA. Blood. 2007; 110:1458-1465.
9. Weis F, Giudice E, Churcher M, Jin L, Hilcenko C, Wong CC, Traynor D, Kay RR, Warren AJ. Mechanism of eIF6 release from the nascent 60S ribosomal subunit. Nat Struct Mol Biol. 2015; 22:914-919.
10. Rujkijyanont P, Watanabe K, Ambekar C, Wang H, Schimmer A, Beyene J, Dror Y. SBDS-deficient cells undergo accelerated apoptosis through the Fas-pathway.

Haematologica. 2008; 93:363-371.
11. Nihrane A, Sezgin G, Dsilva S, Dellorusso P, Yamamoto K, Ellis SR, Liu JM. Depletion of the Shwachman-Diamond syndrome gene product, SBDS, leads to growth inhibition and increased expression of OPG and VEGF-A. Blood Cells Mol Dis. 2009; 42:85-91.
12. Rawls AS, Gregory AD, Woloszynek JR, Liu F, Link DC. Lentiviral-mediated RNAi inhibition of Sbds in murine hematopoietic progenitors impairs their hematopoietic potential. Blood. 2007; 110:2414-2422.
13. Austin KM, Gupta ML, Jr., Coats SA, Tulpule A, Mostoslavsky G, Balazs AB, Mulligan RC, Daley G, Pellman D, Shimamura A. Mitotic spindle destabilization and genomic instability in Shwachman-Diamond syndrome. J Clin Invest. 2008; 118:1511-1518.
14. Orelio C, Verkuijlen P, Geissler J, van den Berg TK, Kuijpers TW. SBDS expression and localization at the mitotic spindle in human myeloid progenitors. PLoS One. 2009; 4:e7084.
15. Sera Y, Sadoya M, Ichinose T, Matsuya S, Imanaka T, Yamaguchi M. SBDS interacts with RNF2 and is degraded through RNF2-dependent ubiquitination. Biochem Biophys Res Commun. 2022; 598:119-123.
16. Sera Y, Imanaka T, Yamaguchi M. M phase-specific interaction between SBDS and RNF2 at the mitotic spindles regulates mitotic progression. Biochem Biophys Res Commun. 2023; 682:118-123.
17. Sera Y, Yamamoto S, Mutou A, Koba S, Kurokawa Y, Imanaka T, Yamaguchi M. *SBDS* Gene mutation increases ROS production and causes DNA damage as well as oxidation of mitochondrial membranes in the murine myeloid cell line 32Dcl3. Biol Pharm Bull. 2024; 47:1376-1382.
18. Yamaguchi M, Fujimura K, Toga H, Khwaja A, Okamura N, Chopra R. Shwachman-Diamond syndrome is not necessary for the terminal maturation of neutrophils but is important for maintaining viability of granulocyte precursors. Exp Hematol. 2007; 35:579-586.
19. Cimini D, Tanzarella C, Degrassi F. Differences in malsegregation rates obtained by scoring ana-telophases or binucleate cells. Mutagenesis. 1999; 14:563-568.
20. Hoyt MA, Totis L, Roberts BT. S. cerevisiae genes required for cell cycle arrest in response to loss of microtubule function. Cell. 1991; 66:507-517.
21. Pachis ST, Kops G. Leader of the SAC: molecular mechanisms of Mps1/TTK regulation in mitosis. Open Biol. 2018; 8:180109.
22. Thornton BR, Toczyski DP. Securin and B-cyclin/CDK are the only essential targets of the APC. Nat Cell Biol. 2003; 5:1090-1094.
23. Novais-Cruz M, Alba Abad M, van IWF, Galjart N, Jeyaprakash AA, Maiato H, Ferras C. Mitotic progression, arrest, exit or death relies on centromere structural integrity, rather than de novo transcription. Elife. 2018; 7:e36898.
24. McAinsh AD, Kops G. Principles and dynamics of spindle assembly checkpoint signalling. Nat Rev Mol Cell Biol. 2023; 24:543-559.
25. Ohshima K, Haraoka S, Yoshioka S, Hamasaki M, Fujiki T, Suzumiya J, Kawasaki C, Kanda M, Kikuchi M. Mutation analysis of mitotic checkpoint genes (hBUB1 and hBUBR1) and microsatellite instability in adult T-cell leukemia/lymphoma. Cancer Lett. 2000; 158:141-150.
26. Ru HY, Chen RL, Lu WC, Chen JH. hBUB1 defects in leukemia and lymphoma cells. Oncogene. 2002; 21:4673-4679.
27. Schnerch D, Schmidts A, Follo M, Udi J, Felthaus J, Pfeifer D, Engelhardt M, Wasch R. BubR1 is frequently repressed in acute myeloid leukemia and its re-expression sensitizes cells to antimitotic therapy. Haematologica. 2013; 98:1886-1895.
28. Havugimana PC, Hart GT, Nepusz T, *et al.* A census of human soluble protein complexes. Cell. 2012; 150:1068-1081.

Received October 2, 2024; Revised October 17, 2024; Accepted October 21, 2024.

**Address correspondence to:*
Tsuneo Imanaka, Laboratory of Physiological Chemistry, Faculty of Pharmaceutical Sciences, Hiroshima International University, Hirokoshingai 5-1-1, Kure, 737-0112, Japan.
E-mail: imanaka@hirokoku-u.ac.jp

Released online in J-STAGE as advance publication October 26, 2024.